CHAPTER 6

MODELING PREDICTIONS AT DIFFERENT GRID SIZES

"In an era that emphasizes global scaled research, data aggregation is widely practiced primarily for "scaling up" environmental analyses or models from local to regional or global scales. Spatial data available at finer resolutions need to be aggregated to represent the spatial characteristics at corresponding scales.

The aggregation process may alter the statistical and spatial characteristics of the data. When aggregated data are used as input to analyses or models, the output of these analyses or models may be affected."

Ling Bian and Rachael Butler, 1999

In this chapter, differences in model predictions due to differences in spatial data aggregation in input grids are studied. As a result of decreasing slope angles defining the terrain at larger spatial resolutions, we expect the predicted erosion rates to decrease, both at the outlet and locally. The first part of this chapter shows that, theoretically, for decreasing averaged slopes, the equilibrium sediment discharge decreases.

First, to isolate the topographic effect on simulated erosion with increasing grid cell size, temporally and spatially uniform rainfall events, uniform impervious soils and uniform land use type are used. Later, the same type of results is shown for a real event case, with spatial and temporal rainfall distribution, and spatial soil type and LULC distribution.

In the USLE equation the length factor, L, is the ratio of field soil loss to the corresponding loss from 72.6-ft (22.1-m) length. In our study, 30-m is chosen to be the reference slope length. The average gross erosion (tons/ha) and sediment yield (tons/ha) are going to be normalized by the corresponding value at 30-m spatial resolution.

6.1. CONCEPTUAL EQUILIBRIUM UNIT SEDIMENT DISCHARGE

Julien and Simons (1984) developed a general sediment transport capacity relationship supported by dimensional analysis. The recommended formula can be written as a power function of slope and discharge, the most significant parameters pointed out by their study:

$$q_s \approx \alpha\, S^{\beta}\, q^{\gamma} \qquad [6\text{-}1]$$

where S is the terrain slope and q is the unit discharge. α, β and γ are empirical exponents. The exponent β varies between 1.2 and 1.9 while the exponent γ varies between 1.4 and 2.4.

In particular, the Kilinc and Richardson equation ($\beta = 1.66$, $\gamma = 2.035$) reveals that predicted erosion rates strongly depend on the hydraulics of the system and the topography. These two factors will be modified with grid aggregation and therefore the prediction of soil erosion will change. Errors in the prediction of the unit discharge or slopes will produce augmented errors in the estimation of the net erosion rates.

Goodwin creek defined at different spatial resolutions (see CHAPTER 4) is used to examine the effects of grid aggregation on the equilibrium sediment discharge. Assuming that this basin is a square watershed at x-m grid cell size with N number of cells and of uniform slope $\overline{So}$ [m m^{-1}] equal to the watershed averaged slope for the given watershed spatial resolution, the length of the watershed is estimated to be:

$$L = \sqrt{N * x^2} \qquad [6\text{-}2]$$

Assuming a uniform constant rainfall intensity, i, impervious condition and uniform LULC and soil type, we can estimate the average equilibrium unit sediment discharge, $\overline{q_s}$, for each grid cell size, x, using a first order approximation to the Taylor Series expansion as:

$$\overline{q_s} = \alpha\,(i * L)^{2.035}\ \overline{So}^{1.66} \qquad \text{or} \qquad \frac{\overline{q_s}}{\alpha} = (i * \sqrt{N} * x)^{2.035}\ \overline{So}^{1.66} \qquad [6\text{-}3]$$

where α is a constant that depends on the soil and land cover.

The mean slopes have been described in section 4.2.1 and they decrease with increasing grid cell size according to the next relationship:

$$\overline{S} = 17.9 * x^{-0.497} \qquad [6\text{-}4\ ]$$

The number of cells defining Goodwin Creek decreases with increasing grid cell size according to the following expression:

$$N = 2E + 07 * x^{-2.012} \qquad [6\text{-}5\ ]$$

Substituting Equations 6-4 and 6-5 into Equation 6-3, we get for the averaged conditions that:

$$\frac{q_s}{\alpha} = 4.14E9 * i^{2.035} * x^{-0.86} \qquad [6\text{-}6\ ]$$

For a given rainfall intensity, i, we can relate the equilibrium unit sediment discharge at x-m grid cell size, qs_x, to a reference equilibrium sediment discharge at 30-m, qs_{30} as follows:

$$\frac{qs_x}{qs_{30}} = \left(\frac{x}{30}\right)^{-0.86} \qquad [6\text{-}7]$$

This is, on the average, as grid cell size, x, increases, the equilibrium unit sediment discharge is expected to decrease.

6.2. MODEL APPLICATION AT DIFFERENT SPATIAL RESOLUTIONS

6.2.1. Method

Uniform Conditions: Spatial and temporal rainfall distributions must be considered as possible sources of error. This error will produce variability in the computed flow (Ogden and Julien, 1993). Thus, temporally and spatially uniform rainfall events have been selected as input to the CASC2D model for testing purposes.

The simulations are carried out using three different constant intensities: 5, 10 and 15mm/h. The rainfall duration was 1200 minutes so that the hydrograph equilibrium conditions are reached for each of the resolutions. The simulation duration was long enough (2500 minutes) to allow for the basin to drain at all resolutions.

The soil parameters are spatially uniform and correspond to the averaged values for a silty-loam soil, the dominant soil type in the watershed. The infiltration and erosion parameter values used in this case are shown in Table 6-1.

Table 6-1. Used soil parameter values for an impervious silty loam soil

SoilType	Drainage condition	Ks [cm/s]	G [cm]	Md [cm^3/cm^3]	K_{USLE}[a]	% Sand[b]	% Silt[b]
Silty loam	Moderate	0	0	0	0.2	20	65

[a]Wischmeier and Smith (1978); [b]USDA (1975) texture triangle

The land use parameters are uniform and correspond to a pasture cover, which represents the largest percentage in the basin. The parameter values used are shown in Table 6-2.

Table 6-2. Used land use parameter values for pasture

Land Cover	Roughness[a]	Interception[b] [mm]	C_{USLE}[b]	P_{USLE}[b]
Pasture	0.2	1	0.02	1

aWoolhiser (1975); bWoolhiser (1990) ; cWischmeier and Smith (1978)

The channels width and depth are described in (section Goodwin Creek experimental watershed). The roughness coefficient for all the channels at all resolutions are kept constant (n=0.0035).

Real Event: The calibration event of October 17, 1981 at 30-m was used to test the effects of grid cell size on the model erosion predictions when spatial variations in soil, land use and rainfall are taken into account.

The model was run at spatial resolution larger than 30-m using the same hydrological parameters. As a result of grid aggregation, peak discharges decrease and times to peak are delayed for the larger grid cell sizes (see Figure 6-1a). The runoff volumes decrease with increasing grid cell size because a lager portion of the water is infiltrated (see Figure 6-1b). Smaller average slopes and progressive vanishing of the larger slopes for the larger grid cell sizes result in a larger opportunity for the water to infiltrate.

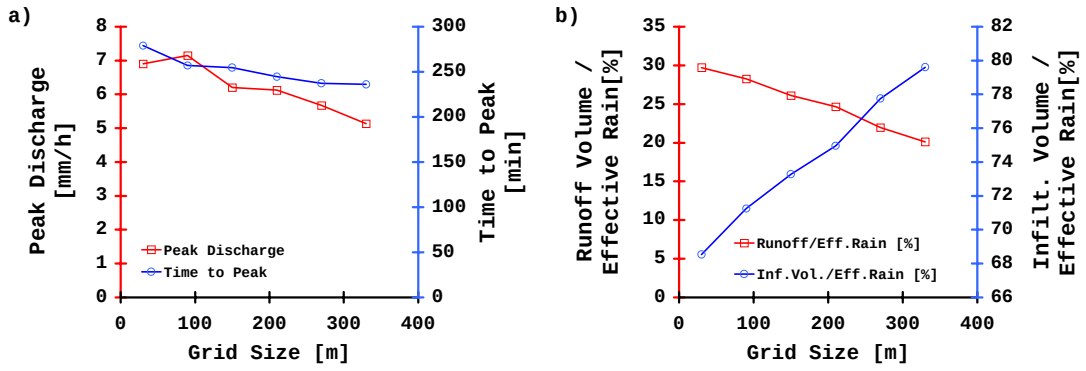

Figure 6-1.a) Peak discharge and time to peak and b) percentage of runoff and infiltration for different grid sizes before model calibration.

The model is then calibrated at spatial resolutions greater than 30-m to get similar peak discharges and runoff volumes at all spatial resolutions by increasing the infiltration rates through the saturated hydraulic conductivity. It is reasonable to assume that flatter

slopes would lead into more saturated areas in the watershed, and thus, the moisture deficit has been reduced for increasing grid cell sizes. Finally, the channels roughness coefficient has been increased with increasing grid cell sizes to cause a delay in the hydrograph peak. After calibration, the new peak discharges, time to peak, and percentages of runoff and infiltration volumes are shown in Figure 6-2a,b.

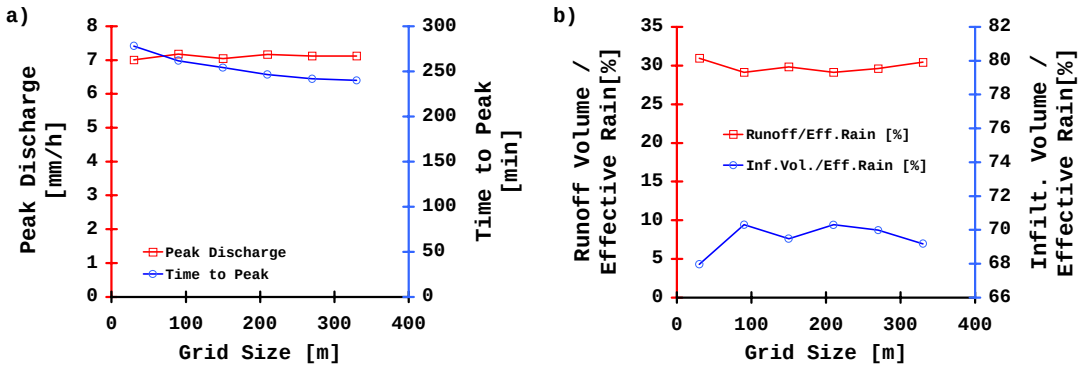

Figure 6-2. a) Peak discharge and time to peak and b) percentage of runoff and infiltration for different grid sizes

An increase in the grid cell size tend to decrease the basin's average slope and slope range thus creating a milder runoff surface, and, in turn, reducing simulated water depths. As already shown in the last section, reducing the water depth will induce a reduction in the transport capacity as calculated by the Kilinc and Richardson equation by reducing the unit discharge. This is, the reduction in the slope with increasing grid cell sizes will affect the transport capacity both directly, through the slope, S, term, and indirectly, through the unit discharge term, q.

6.2.2. Results

Equilibrium Unit Sediment discharge: In the case of uniform rainfall conditions, a regression line has been fitted to the simulated equilibrium sediment discharge values normalized by the respective value at 30-m spatial resolution for each rainfall intensity.

This equation is similar to the empirical one (Equation 6-7) obtained for the averaged conditions.

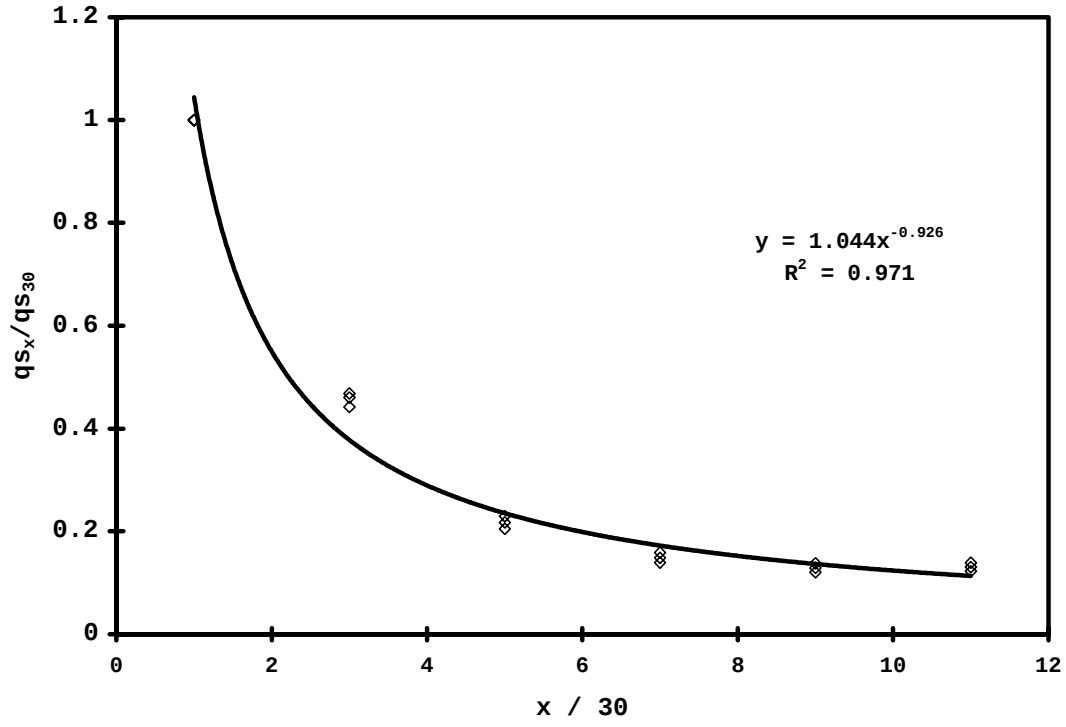

Figure 6-3. Normalized equilibrium sediment discharge at the watershed outlet for different normalized grid cell values and rainfall intensities.

Average gross erosion and average sediment yield: Average gross erosion is defined as the volume of parent material per unit area [tons ha^{-1}] that has been scoured in the basin, without taking into account deposition. Average sediment yield is defined as the amount of sediment per unit area [tons ha^{-1}] leaving the watershed. Both quantities have been normalized at all spatial resolutions by the respective amount obtained at the 30-m simulations. Figure 6-4 shows the normalized average gross erosion and sediment yield for the case of uniform rainfall (with 5, 10 and 15 mm/h intensity), soil type and LULC. Figure 6-5 shows the same results for the distributed conditions case. As

expected, simulated erosion values decrease with grid cell size with the strongest dependency found for the case of the averaged gross erosion.

The normalized averaged gross erosion in the case of the uniform and the distributed conditions are practically identical. The next approximate regression line is fitted to the model simulated values in both cases:

$$\frac{\overline{E}_x}{\overline{E}_{30}} = 170 * x^{-1.5} \qquad [6\text{-}8]$$

where

E_x = gross erosion simulated at x-m [tons ha^{-1}]
E_{30} = gross erosion simulated at 30-m [tons ha^{-1}]
x = grid cell size [m]

For the averaged conditions, if the slope decreases with the inverse of the squared root of the cell size (Equation 6.4), then the unit discharge should decrease with the inverse of the cubic root of the cell size as shown in the next expression:

$$\left.\begin{aligned} \frac{\overline{E}x}{\overline{E}_{30}} &\propto \left(\left(\frac{x}{30}\right)^{-0.5}\right)^{1.66} * \left(\left(\frac{x}{30}\right)^{a}\right)^{2.035} \\ \frac{\overline{E}_x}{\overline{E}_{30}} &\propto x^{-1.5} \end{aligned}\right\} \Rightarrow \quad a \cong -1/3 \qquad [6\text{-}9]$$

Thus, on the average, the unit discharge also depends on the grid cell size although the effect of the changes in slope values with grid cell sizes in the transport equation will be larger.

The averaged sediment yield takes into account not only the amount of sediment eroded in the watershed but also deposition. Thus, a change in grid cell size will affect less the model sediment yield predictions than it does the gross erosion (see Figure 6-4

and Figure 6-5). For the smaller spatial resolution models, sediment deposits on concave areas or areas of low slope. As the grid spatial resolution increases, a) the convexities and concavities of the terrain tend to disappear and thus the rates of local erosion and deposition, respectively, decrease and b) slope lengths become shorter and the channels become less sinuous which causes a faster routing of the sediment to the outlet.

The normalized averaged sediment yield is affected by the spatial variability of the rainfall, soils and land use input. The regression line fitted for the uniform and spatially variable cases are (also shown in Figure 6-4 and Figure 6-5):

$$\left[\frac{Y_x}{Y_{30}}\right]_{UniformConditions} = 32.2 * x^{-0.995}$$

$$\left[\frac{Y_x}{Y_{30}}\right]_{Spatial\ variability} = 50.8 * x^{-1.153}$$

This is, spatial variabilities will increase the difference in the sediment yield predictions between the model at certain spatial resolution, x-m, and the reference one, 30-m. Resampling of the soil type and land use grids to coarser resolution affects the sediment yield prediction by affecting deposition patterns

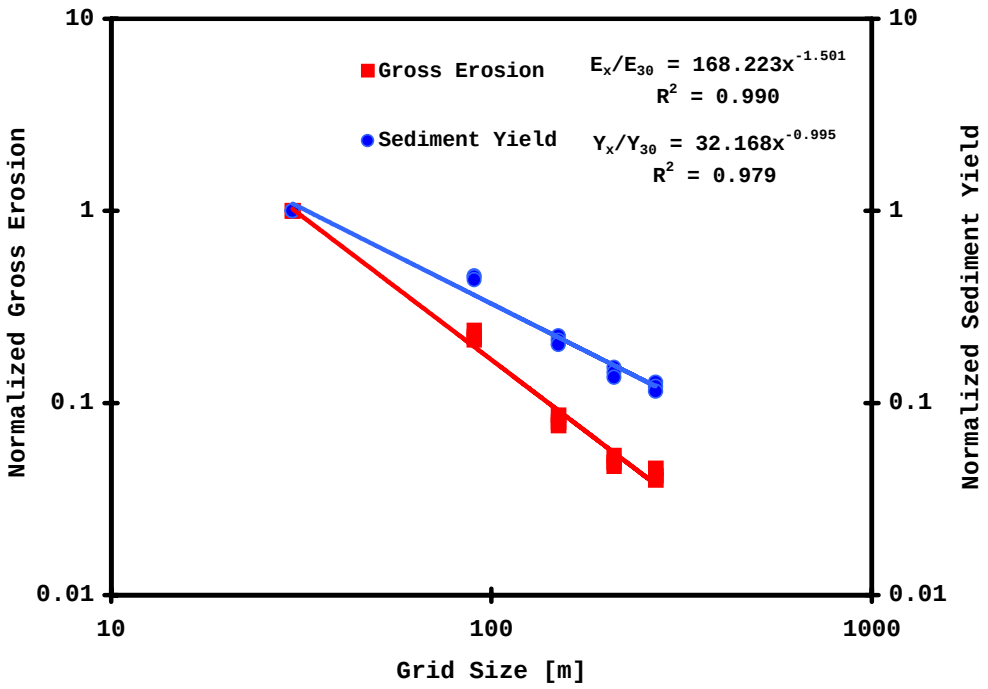

Figure 6-4. Normalized averaged gross erosion and sediment yield for the uniform conditions case.

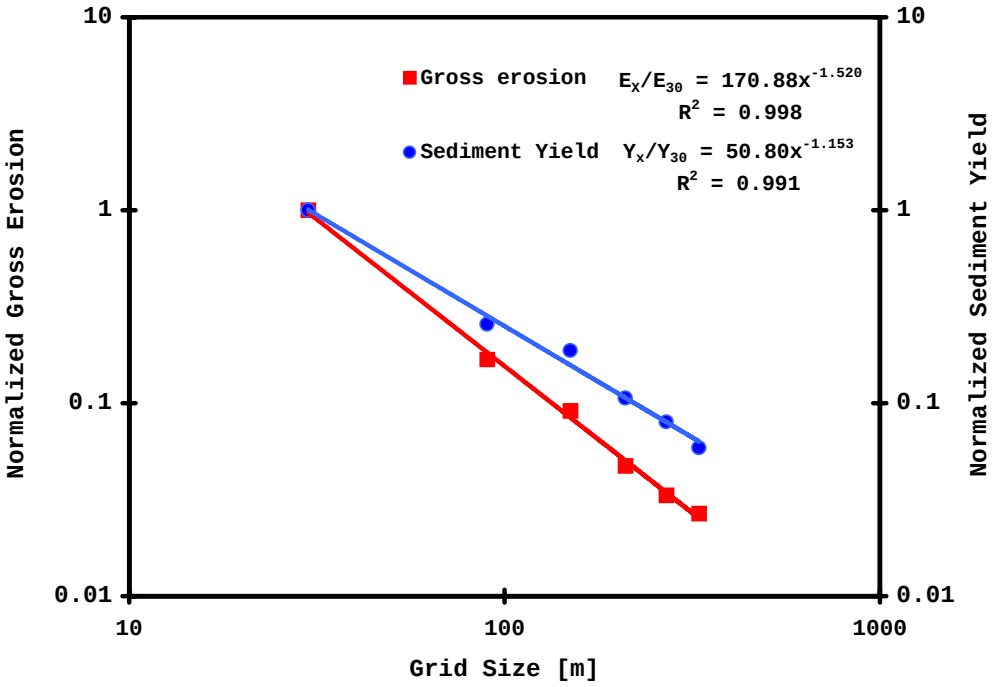

Figure 6-5. Normalized averaged gross erosion and sediment yield for the distributed conditions case.

Net erosion volumes: Net erosion values are the result of adding deposited volumes (positive quantity) and scoured volumes (negative quantity) of sediment at a given grid cell. Spatially, net erosion volumes change depending on the input grid spatial resolution as shown in Figure 6-7 (uniform conditions with 15 mm/h rainfall intensity) and Figure 6-8 (distributed conditions). The net erosion pattern also change with the distributions of soil and land use (compare Figure 6-7 and Figure 6-8).

Visual inspection of the net erosion maps indicates that the 30-m resolution grid is the one simulating net erosion values closer to reality while the 330-m does not perform as well. Figure 6-6a represents the percentage of the watershed area suffering either net erosion, deposition or zero net erosion as seen in Figure 6-7. Figure 6-6b represents the percentage of the watershed area suffering either net erosion, deposition or zero net erosion in Figure 6-8. In Figure 6-6a, the 30-m grid is the one has the largest area covered by net deposition (28%) and the smallest area in which the net erosion is zero (5%) while in the 330-m grid the opposite happens (10% with net deposition and 25% with no net erosion). The largest percentage of net erosion has a maximum on the 150-m grid. In Figure 6-6b, the trends are similar to those in the uniform conditions case, where the 30-m grid has the largest percentage of the area covered by net deposition and the coarsest resolutions have the largest percentage of the area in which the net erosion is zero. The 90-m grid has maximum percentage of the area covered by net erosion

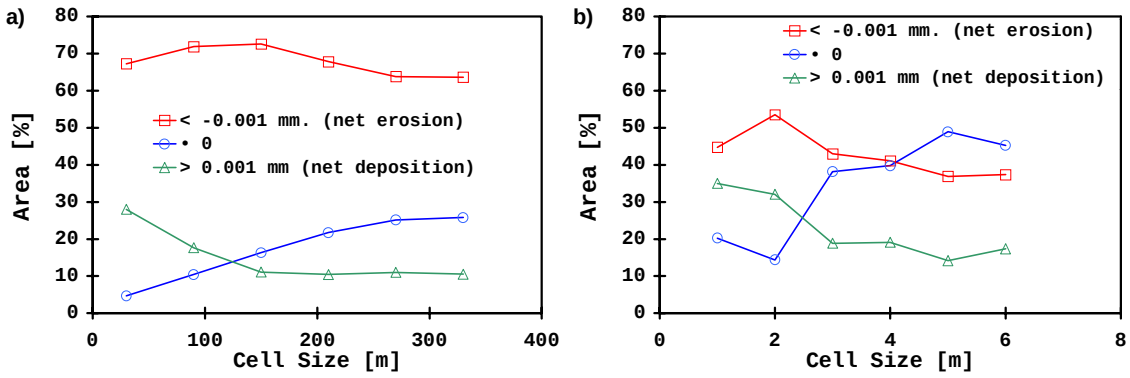

Figure 6-6. Percentage of the watershed with net erosion, deposition, and zero net erosion for the case a) of the uniform conditions (15 mm/h rainfall intensity) and b) distributed conditions (event 1)

Location of the sediment source and deposition areas, and volume of sediment eroded transported and delivered are some of the factors that should be quantified before deciding what erosion control treatment is best suited for a problem. In this case, it seems advisable to recommend that simulations with the smaller grid cell sizes are carried out.

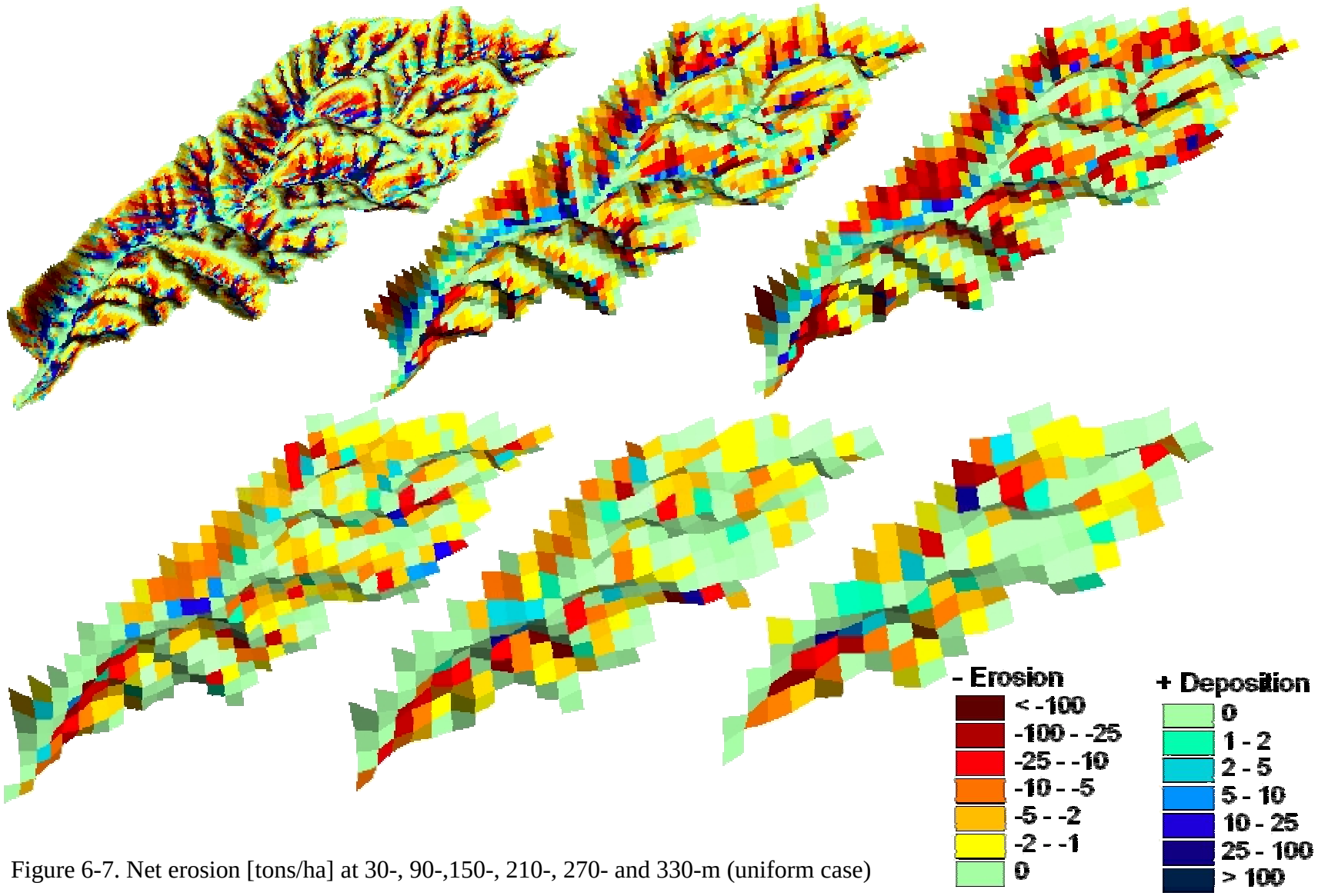

Figure 6-7. Net erosion [tons/ha] at 30-, 90-,150-, 210-, 270- and 330-m (uniform case)

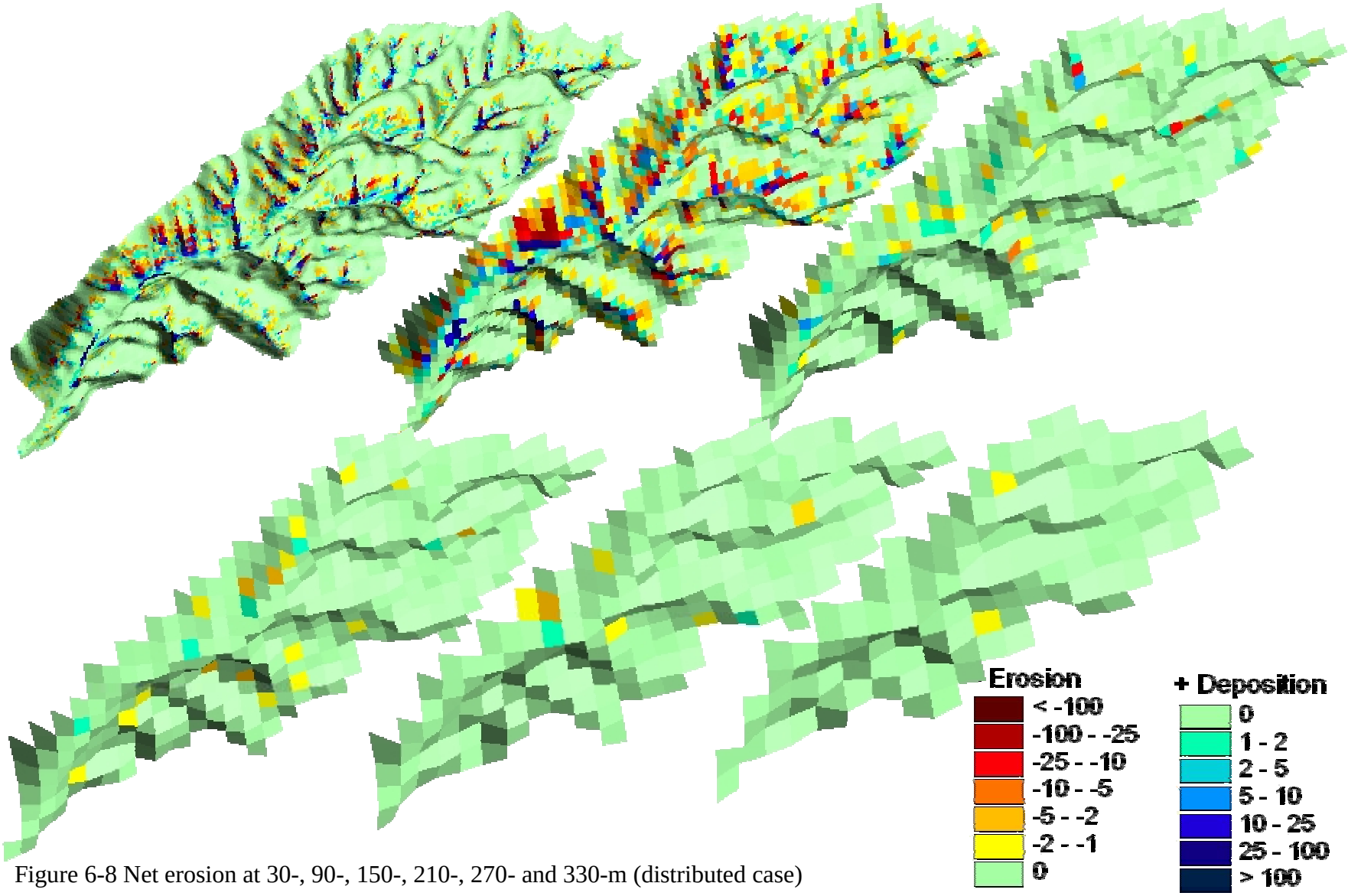

Figure 6-8 Net erosion at 30-, 90-, 150-, 210-, 270- and 330-m (distributed case)

Sediment delivery ratio (SDR): The SDR denotes the ratio of the sediment yield at a given stream cross section to the gross erosion from the watershed upstream from the measuring point. The SDR depends primarily on the drainage area of the upstream watershed (Julien, 1995). Figure 6-9a and Figure 6-10a show the SDR obtained for the case of the uniform conditions and for the case of the distributed ones, respectively. Figure 6-9b,c,d and Figure 6-10b,c,d show the SDR for the particular case of the sand, silt and clay fractions, respectively.

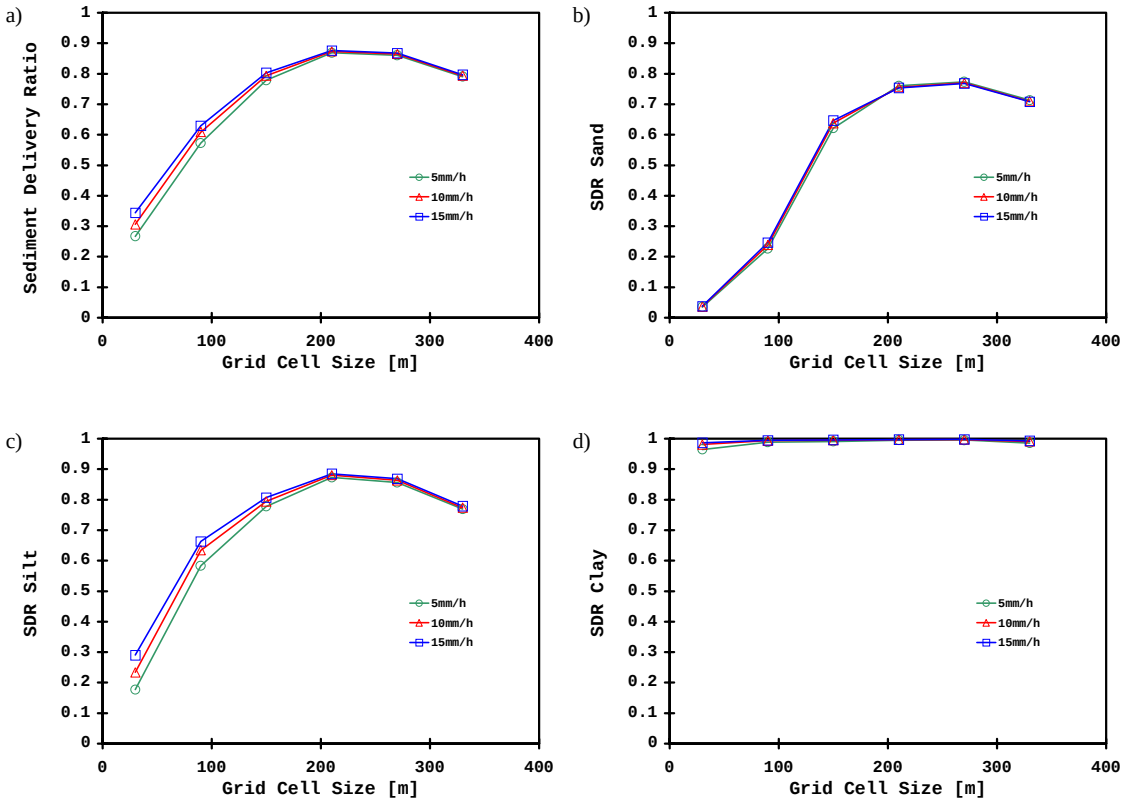

Figure 6-9. Sediment delivery ratio of Goodwin creek watershed for a) total sediment load, b) sand load, c) silt load and d) clay load as a function of grid size and rainfall intensity for the uniform case.

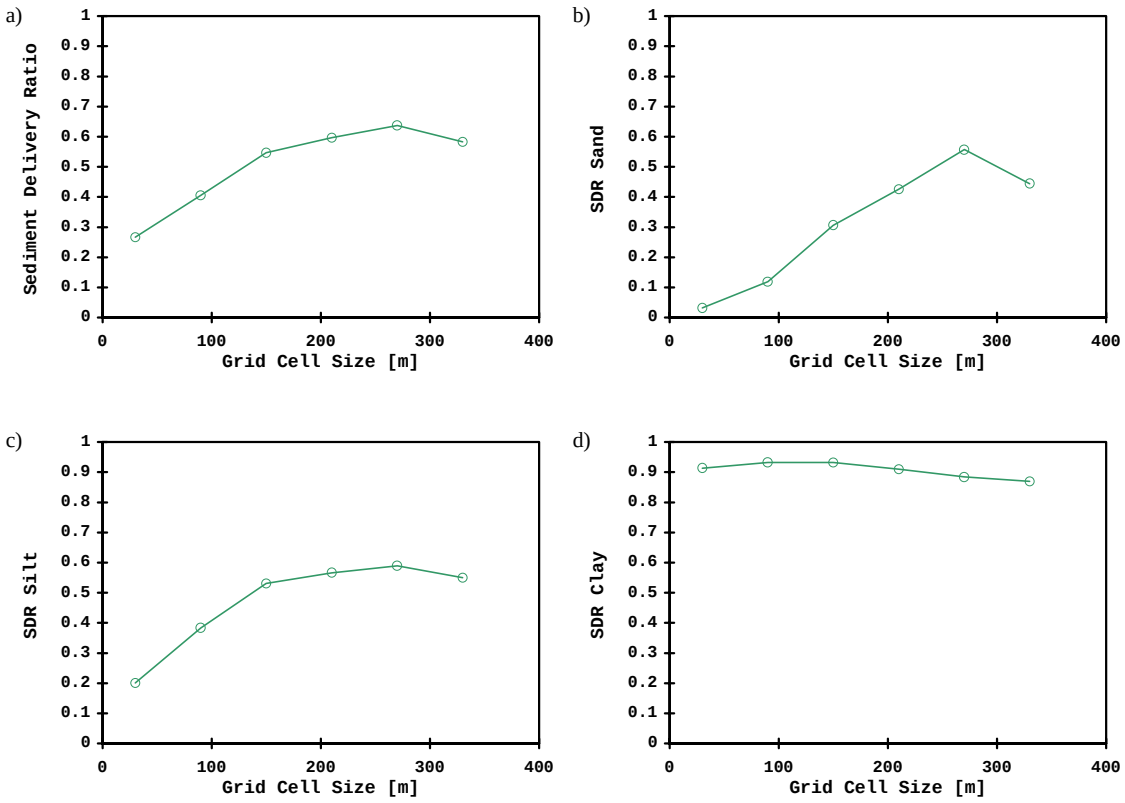

Figure 6-10. Sediment delivery ratio of Goodwin creek watershed for a) total sediment load, b) sand load, c) silt load and d) clay load as a function of grid size for the distributed case.

The distribution of the SDR of sand and clay does not change much with rainfall intensity (see Figure 6-9b,d). The reason why this happens is that the sand fraction moves mostly as bed material and the clay as suspended load due to their large and very small settling velocities, respectively. In the case of the silt (Figure 6-9c) the rainfall intensity or, equivalently, the water discharge affects its transport rate. With larger water depths for the larger rainfall intensity, larger fraction of the silt will move as suspended sediment and thus, for the same spatial resolution, the fraction of silt leaving the basin increases for larger rainfall intensities. The small differences in the SDR with precipitation intensity are due to differences in the transport of the silt fraction.

Basically, the SDR for the distributed conditions case follows the same pattern as the one for the uniform conditions although the range of variation of the SDR with grid cell size is smaller in the first case.

Sediment delivery ratios increase with grid cell size up to the 210-m grid in the case of the uniform conditions. As shown in Figure 6-9, for grid sizes 210-m or larger, the net soil loss area starts decreasing and the area of zero net erosion increases while the area of net deposition is maintained. This induces a reduction in the SDR values for grid sizes larger than 210-m. In the case of the distributed conditions, SDRs increase up to the 270-m grid (see Figure 6-10). It should be noted that the sum of areas with net erosion and the areas of zero net erosion has a maximum at the 210-m grid in the case of the uniform conditions and 270-m grid in the case of the distributed conditions.

According to Boyce (1975), the SDR for a drainage basin of 20.5 km^2 (7.9 mi^2) has been observed to vary between 0.1 and 0.5. Figure 6-11 shows the SDR values of the simulated event 1 (from 30- to 330-m) and events 2 and 3 (at 90-m) superposed with the Boyce data. Falling within the range of observed data, the SDRs simulated for the case of the 30- and 90-m grid cell size are comparable to field observations. SDRs for larger grid cell sizes greater are overpredicted.

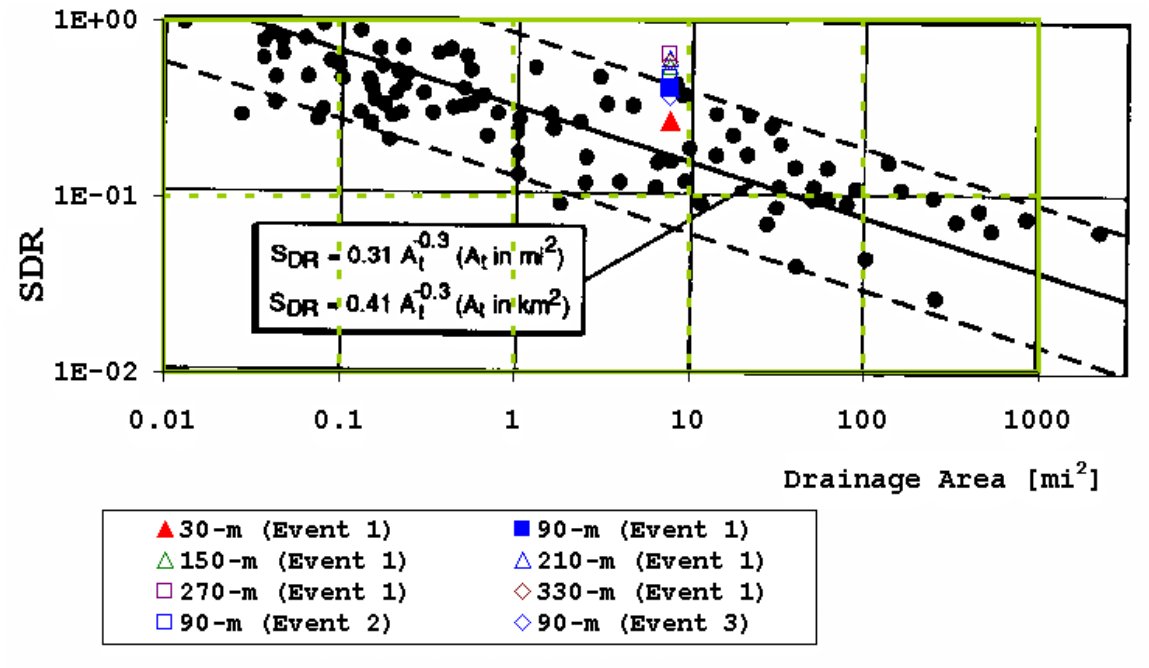

Figure 6-11. Boyce observed sediment delivery ratio values and simulated ones with CASC2D-SED

6.3. SUMMARY

Differences in model erosion predictions due to differences in spatial data aggregation in input grids have been studied for two different cases. In the uniform conditions case, rainfall intensity, soil type and land use type are maintained uniform. In the distributed conditions case, an observed rainfall event, and distributed soil and land use types have been used. The following has been shown:

(1) Empirical and simulated equilibrium sediment discharge at spatial resolution x is related to the value simulated at 30-m spatial resolution approximately according to the following equation:

$$\frac{qs_x}{qs_{30}} = \left(\frac{x}{30} \right)^{-0.9}$$

(2) Gross erosion depends, among others, on terrain slope and unit discharge, with the stronger dependency on the first one. The normalized gross erosion decreases with $x^{-1.5}$, with x representing the grid cell size.

(3) Predicted sediment yield values are less sensitive to the model grid cell size than gross erosion predictions because it takes into account not only erosion but also deposition rates. The normalized sediment yield decreases approximately with the inverse of the grid cell size. Resampling of the soil type and land use grids affects simulated averaged sediment yield.

(4) Spatially, net erosion volumes change depending on the input grid cell size. The area covered with net deposition decreases while the area with zero net soil erosion increases. These values affect in turn the sediment delivery ratio (SDR). Simulated values for the smaller grid cell sizes (30-m to 150-m) represent erosion and deposition patterns more realistically than the coarser resolution grids.

(5) SDRs increase with increasing grid cell size. SDRs are not greatly affected by the rainfall intensity. Differences in the SDR for the smaller spatial resolutions are due to differences in the silt SDR. The SDR simulated for the case of the 30- and 90-m grid cell size for the uniform conditions and the distributed conditions fall within observed SDR range by Boyce (1975) for the Goodwin Creek drainage area.